HYDRAULIC DRAG AND STRUCTURE OF GAS-LIQUID MIXTURE PLUG FLOW IN HORIZONTAL AND NEARLY HORIZONTAL TUBES

É. É. Markovich

UDC 532.529

Based on an analysis of plug flow structure with the use of mass and momentum conservation equations, relations for describing hydraulic drag in horizontal and slightly inclined tubes have been obtained.

One of the most important parameters employed for calculating pipelines is the pressure drop along a tube resulting from hydraulic resistance. The determination of the pressure drop in horizontal tubes with gas-liquid mixture plug flow is partially or totally the subject of many investigations carried out over several decades ([1-8], etc.). A great deal of experimental information has been accumulated. However, on the whole the results cannot be regarded as fully satisfactory, because a multitude of computational techniques are available that differ not only in the quantities being determined and their magnitudes, but also in the effect of different factors on pressure drop along a tube (see, for example, the review [9]).

In the present paper it will be shown that if we resort not to available formulas but directly to experimental data obtained by various authors and reduce them all to a single form, then almost all of the experimental data accumulated for decades fall on a single curve with a standard deviation of mean values from different sources amounting to 0.06.

A plug flow in a tube constitutes a sequence of moving plug cells (1) (Fig. 1) each of which consists of a liquid plug (2) occupying the whole cross section of the tube, a gas bubble (3) which occupies a portion of the tube cross section and which is located between two neighboring plugs, and a liquid layer (4) which underlies the bubble and is adjacent to the tube wall. The lengths of the plugs and bubbles are much larger than the tube diameter. The motion in the plug, the bubble, and the layer is close to one-dimensional. The transition between the layer and the plug takes place over non-one-dimensional, but short, stretches called the leading (5) and trailing (6) fronts of the plug. The fronts move faster than the liquid in the plug. Therefore, in the front the plug rolls onto the layer and absorbs it, while at the rear the plug leaves a liquid which forms a new layer. The gas in the bubble moves with the front velocity C, i.e., faster than the liquid in the plug, and causes the slippage of phases. The slippage of phases is characterized by the ratio χ of the mean-flow velocity W (equal to the mean-flow velocity of liquid in the plug) to the velocity of the gas (and of the fronts) C [10].

In a steady-state flow the ratio χ is entirely determined by the motion of liquid at the trailing front, since, by the mass conservation law (from the balance of liquid flow rates), the velocities of the leading and the trailing fronts are equal. Experience and analysis show [11] that there are two regimes of motion of the trailing front: the gravitational regime, when the front velocity and the thickness of the layer remaining behind it are governed by the velocity of liquid flow from the upper point of the front over the phase interface surface under the action of gravity; and the kinematic regime, when the flow velocity is very small, the front velocity becomes equal to the maximum liquid velocity in the plug, and the layer thickness behind the front is governed by the equalization of the liquid velocity profile from tubular in the plug to uniform in the layer.

In Fig. 2 experimental data are presented on the trailing front velocity obtained in a 56-mm-diameter tube on a water-air system (light points) and on a system of oil and oil gas at a pressure of about 4 MPa in a 100-mm-diameter tube (dark points). With Froude numbers $Fr < 3.3$, the motion regime is gravitational and the parameter χ depends on the Froude number. At large Froude numbers the regime is kinematic and, since the flow is turbulent, $\chi \approx 0.82 = \text{const}(Fr)$ (straight line 1). The function $\chi = \chi(Fr)$ for the gravitational regime is amenable to calculation on the basis of conservation laws according to the method suggested in [12]. The results of calculation are presented by curve 2. Since for the aims of the present paper it is sufficient to know only the function $\chi = \chi(Fr)$ per se, the calculation will not be given here, but both the experimental and predicted data on the trailing front velocity will merely be expressed by an empirical formula akin to that of Mamaev [13]:

Krasnodar Polytechnic Institute. Translated from Inzhenerno-Fizicheskii Zhurnal, Vol. 62, No. 6, pp. 792-802, June; 1992. Original paper submitted April 6, 1988.

1062-0125/92/6206-0568$12.50 ©1992 Plenum Publishing Corporation

$$\chi = 0{,}82\,(1 - \exp\,(-\,1{,}9\,\sqrt{\mathrm{Fr}}\,)) \tag{1}$$

(curve 3).

Calculation of pressure drop in a tube with a plug flow should be naturally carried out for one plug cell. The pressure drop across a plug cell is composed of the pressure drop Δp_f across a liquid plug and Δp_g across a gas bubble. The motion is assumed to be steady.

The pressure drop across a liquid plug Δp_f will be calculated using momentum and mass conservation laws for a liquid test volume bounded by the tube walls, transverse cross sections 1 and 2 (see Fig. 1), and by the phase interface surface at the leading and trailing fronts. The test volume moves along the tube with the velocity of the fronts, and it will be considered in the coordinate system moving together with it.

The momentum equation projected along the tube axis for the test volume has the form

$$F_{fa} + F_{fb} + F_{fc} + F_{fd} = 0, \tag{2}$$

where

$$F_{fa} = \int_S p_2 dS_2 - \int_S p_1 dS_1 \tag{3}$$

is the longitudinal pressure force acting on the plug,

$$F_{fb} = -\lambda \frac{L_f}{D} \frac{\rho_f W^2}{2} S \tag{4}$$

is the frictional force on the tube walls,

$$F_{fc} = -\rho_f g \sin\gamma\, L_f S \tag{5}$$

is the longitudinal component of gravity acting on the test liquid volume provided that the lengths of the fronts are small,

$$F_{fd} = \rho_f V S\,(V_2 - V_1) \tag{6}$$

is the longitudinal momentum flux through the test volume. The liquid mass conservation equation for the test volume has the form

$$VS = V_1 S_1 = V_2 S_2. \tag{7}$$

An expression for pressure at any point of the cross section i (i = 1, 2) will be obtained by assuming that pressure distribution is hydrostatic, whereas the phase interface surface is cylindrical with a horizontal generatrix perpendicular to the tube axis:

$$p_i = p_{i0} + \rho_{gi} g \cos\gamma\,(D - H_i) + \rho_f g \cos\gamma\,(H_i - y). \tag{8}$$

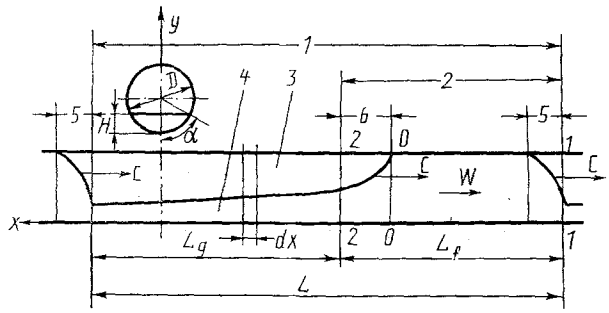

Fig. 1. Scheme of plug flow.

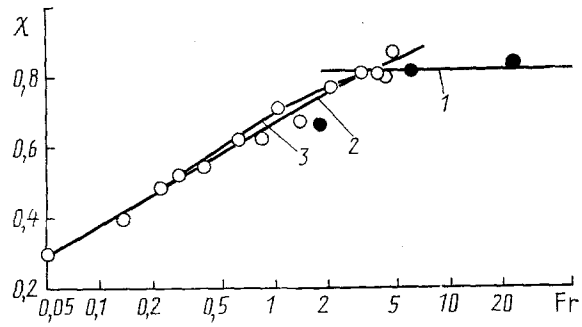

Fig. 2. Ratio of mean-flow velocity to the velocity of fronts in horizontal-tube plug flow.

For a circular tube (see Fig. 1)

$$\int_S p_i dS = p_{i0} S + \rho_{gi} g \cos\gamma \frac{DS}{2} + (\rho_f - \rho_{gi})\, g \cos\gamma\, DS\Phi_i, \tag{9}$$

$$\Phi_i \equiv \frac{\sin^3\alpha}{3\pi} - \frac{a_i \cos\alpha_i}{2}. \tag{10}$$

Neglecting the difference in the gas densities in front of the plug and behind it, i.e., assuming that $\rho_{g1} = \rho_{g2} = \rho_g$, assuming that the pressure drop across the plug is calculated near the upper generatrix of the tube, i.e.,

$$\Delta p_f = p_{20} - p_{10}, \tag{11}$$

and substituting Eq. (9) into Eq. (3) yield

$$F_{fa} = \Delta p_f S + DS\,(\rho_f - \rho_g)\, g \cos\gamma\,(\Phi_2 - \Phi_1). \tag{12}$$

Now, the momentum flux (6) will be calculated using the coupling between the absolute and relative mean-flow velocities

$$V = (1/\chi - 1)\, W \tag{13}$$

TABLE 1. Experimental Conditions in the Determination of Pressure Drop in Plug Flow in Horizontal Tubes

Designations in Fig. 4 and referenced	Re	Fr	ρ	D, b.	Mixture
1 [1]	$2\cdot10^4$—$4\cdot10^5$	2—1000	$0(10^{-3})$	26	Water–air
2 [2]	$6\cdot10^5$	2,4	$7\cdot10^{-2}$	197	Oil–oil gas
3 [3]	10^5—10^6	3—300	$4\cdot10^{-3}$ $4\cdot10^{-2}$	101,152	Water–air
4 [4]				101,152	Water–natural gas
5 [5]	$5\cdot10^3$—$2{,}5\cdot10^5$	2—50	$0(10^{-3})$	50	Water–air
6 [6]	$7\cdot10^4$—$8\cdot10^5$	4—500	$(1$—$5)\cdot10^{-3}$	50	Water–air
7 [7]	$0(10^5)$	4	$0(10^{-3})$	50	Water–air
8 [8]	$2\cdot10^4$—$5\cdot10^5$	2—200	$0(10^{-3})$	45	

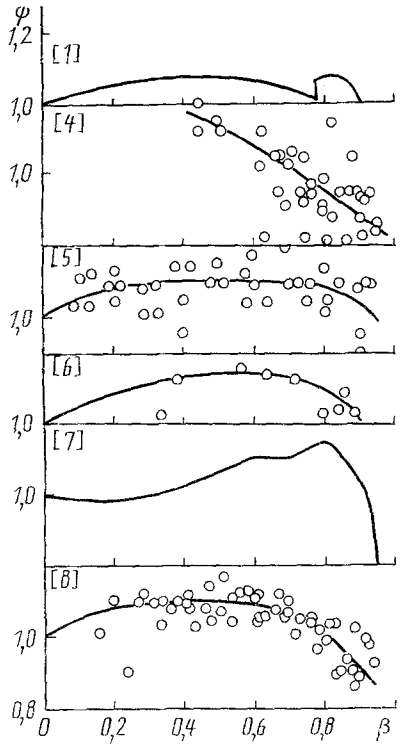

Fig. 3. Experimental data on pressure drop in horizontal-tube plug flow.

and mass conservation law (7). This gives

$$F_{fd} = \rho_f W^2 S\,(1/\chi - 1)^2\,(1/a_2 - 1/a_1). \tag{14}$$

Substituting Eqs. (4), (5), (12), and (14) into the momentum conservation equation (2) and solving it for Δp_f yield

$$\Delta p_f = \lambda \frac{L_f}{D}\frac{\rho_f W^2}{2} + L_f \rho_f g \sin\gamma - \rho_f W^2 \left(\frac{1}{\chi} - 1\right)\left(\frac{1}{a_2} - \frac{1}{a_1}\right) - \\ - D\,(\rho_f - \rho_g)\,g\cos\gamma\,(\Phi_2 - \Phi_1). \tag{15}$$

In the coordinate system adopted, the mean-flow velocity in all the cross sections of the gas bubble is equal to zero; therefore, momentum flux is also absent. The momentum conservation law transforms into a force balance equation. Select a

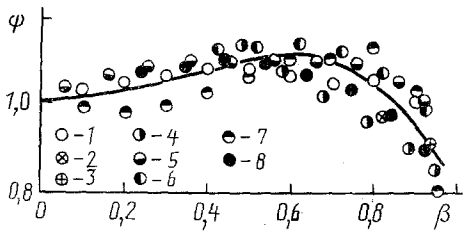

Fig. 4. Averaged experimental data on pressure drop in plug flow through horizontal tubes (for designations see Table 1).

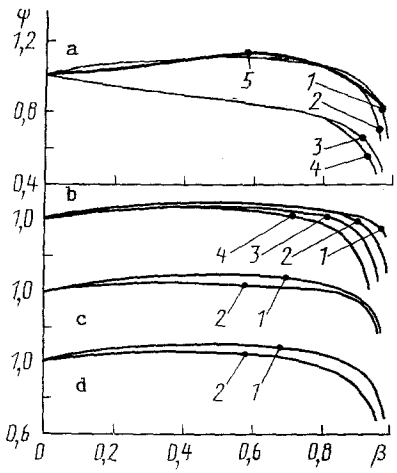

Fig. 5

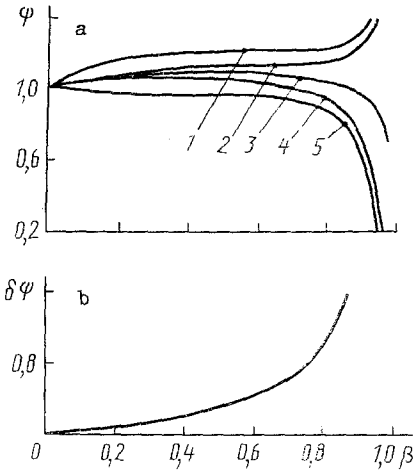

Fig. 6

Fig. 5. Comparison between predicted and experimental data on pressure drop in plug flow through horizontal tubes.

Fig. 6. Effect of deviations from horizontal position on pressure drop in plug flow in tubes ($\gamma = \pm 0.01$).

test volume in the form of a thin gas layer of thickness dx (Fig. 1) cut out by two closely spaced cross sections, bounded on the sides by the tube wall and phase interface surface (liquid layer boundary).

After suitable transformations the pressure drop across the bubble takes the form

$$\Delta p_g = \int_0^{L_g} dp_g = \Delta p_1 + \Delta p_2 + \rho_g g \sin \gamma L_g, \tag{16}$$

where

$$\Delta p_1 = \int_0^{L_g} \lambda_1 \frac{\rho_g C^2}{2} \frac{dx}{4(1-a)S/\Pi_g}, \tag{17}$$

$$\Delta p_2 = \int_0^{L_g} \lambda_2 \frac{\rho_g (w_g - w_f)^2}{2} \frac{dx}{4(1-a)S/\Pi_{fg}}. \tag{18}$$

The liquid layer under the gas bubble does not directly enter into the calculation of the pressure drop, since, because of the one-dimensionality of motion, the pressure drop across it is the same as across the bubble. However, the layer parameters (length L_g, fraction of the cross-sectional area occupied by it a, phase interface surface width Π_{fg}, mean velocity at the interface w_f) enter into the formulas for the pressure drop. Therefore, calculation of the liquid layer is necessary.

The calculation will be carried out using both the momentum and mass conservation laws for a test volume cut out of the liquid by two adjacent cross sections a distance of dx apart (Fig. 1) and bounded on the sides by the tube wall and phase interface surface, which, just as in sections 2 and 3, is assumed to be cylindrical with a horizontal generatrix.

The momentum equation for the layer, after division by the tube cross-sectional area S, takes the form

$$\rho_f q \frac{d(W_f - c)}{dx} dx = -\frac{dp_g}{dx} a dx - (\rho_f - \rho_g) g a \cos\gamma \, dH - \\ - \lambda_f \frac{\rho_f |W_f| W_f}{2} \frac{\Pi_f}{4S} dx - \lambda_2 \frac{\rho_g |w_g - w_f| (w_g - w_f)}{2} \frac{\Pi_{fg}}{4S} dx, - \rho_f g a \sin\gamma \, dx, \tag{19}$$

where

$$q = (W_f - C) a \tag{20}$$

is the liquid flow rate through the layer cross section. The left-hand side of Eq. (19) contains the momentum flux, whereas its right-hand side involves (in order): pressure force generated by pressure drop at the upper generatrix of the tube; pressure force brought about by the change in the layer height; force of layer friction against the tube wall; force of layer friction against the gas on the phase interface surface; longitudinal component of the gravitational force acting on the layer. The pressure drop dp_g is found from the equation for the bubble (16). Pressure distribution in all the cross sections is assumed to be hydrostatic.

The mass conservation law for the test volume is

$$C - W = a(C - W_f) \tag{21}$$

or in dimensionless form

$$1 - \chi = a(1 - \theta). \tag{22}$$

Using the geometric relationship

$$\Pi_{fg} dH = S da \tag{23}$$

and the mass conservation law and writing Eq. (19) in a dimensionless form gives

$$\frac{d\xi}{da} = \frac{z_1}{z_2}, \tag{24}$$

where the numerator is given by

$$z_1 = -(1 - \theta)^2 + \frac{a}{i_{fg}} \chi^2 \frac{(1 - \rho)\cos\gamma}{\mathrm{Fr}}, \tag{25}$$

and the denominator is given by

$$z_2 = \frac{\lambda_1}{2}\rho\frac{a_{ig}}{1-a} + \frac{\lambda_2}{2}\rho|K_g - K_f\theta|(K_g - K_f\theta) - \tag{26}$$

$$-\frac{\lambda_f}{2} i_f |0| \theta - a\chi^2 \frac{(1-\rho)\sin\gamma}{\mathrm{Fr}},$$

$$a = \frac{1}{\pi}\left(\alpha - \frac{\sin 2\alpha}{2}\right);\ i_f = \frac{\alpha}{\pi};\ i_g = \frac{\pi-\alpha}{\pi};\ i_{fg} = \frac{\sin\alpha}{\pi}. \tag{27}$$

Using Eqs. (22) and (24) it is possible, by numerical calculation, to find the change in the dimensionless area and in other parameters of the layer along the tube. For this it is necessary to assign the friction coefficients λ_1, λ_2, and λ_f and also the coefficients

$$K_g = w_g/C,\ K_f = w_f/C. \tag{28}$$

By assuming that the flow near all the boundaries is the same as at the wall in a tube with a single-phase flow, we can consider that $K_g = K_f = 1$ and that

$$\lambda_1 = \lambda_1(\Delta,\ \mathrm{Re}_1);\ \lambda_2 = \lambda_2(\Delta,\ \mathrm{Re}_2);\ \lambda_f = \lambda_f(\Delta,\ \mathrm{Re}_f) \tag{29}$$

are determined from ordinary hydraulic relations. Here

$$\mathrm{Re}_1 = \frac{\rho_g C}{\mu_g}\left(\frac{4S(1-a)}{\Pi_g}\right);\ \mathrm{Re}_2 = \frac{\rho_g(C-W_f)}{\mu_g}\left(\frac{4S(1-a)}{\Pi_{fg}}\right);\quad \mathrm{Re}_f = \frac{\rho_f|W_f|}{\mu_f}\left(\frac{4Sa}{\Pi_f}\right). \tag{30}$$

It will be clear from the further discussion that some of the assumptions adopted are incorrect, because the results of calculations turn out to be far from those obtained experimentally. The best agreement with the experiment is obtained when twice as large a value of the coefficient λ_f as that used in hydraulic relation (29) is used, while the friction force on the phase interface surface is taken to be equal to zero. Let us clarify the reason for the discrepancy.

It is known [14] that in the case of longitudinally uniform flow of liquid layers in tubes and channels, the actual friction coefficient may exceed that calculated by analogy with a filled tube by no more than a few percent. Consequently, the reason for the discrepancy is the fact that the longitudinal motion of the layer is nonuniform.

In the adopted coordinate system, in which the motion of the layer is stationary, the layer is accelerated due to the friction on the tube wall moving with the velocity of the fronts C. At all times, the wall sheds additional vorticity to the layer. If it is assumed that the identical vorticity is immediately damped by the internal friction in the fluid, then the motion in the layer should be the same as in a filled tube where the vorticity balance is maintained. If this is not the case, strong secondary flows should originate in the layer.

It is known that, even with longitudinally uniform motion in layers with a free surface, strong secondary flows [15, 16] originate, under the action of which the maximum of the longitudinal velocity is located not at the free surface, but in the interior of the layer, and the velocity decreases in approaching the free surface in spite of the fact that friction there is very small. A similar conclusion for a liquid layer in plug flow follows from the results of work [17].

This phenomenon can be understood if it is assumed that the vorticity supplied from the wall to the layer is damped slowly. In this case, in accordance with the law of conservation of angular momentum, simultaneously with the arrival of vorticity from the wall, there should originate within the layer a compensating vorticity similar to an accelerated vortex in wing acceleration. By assuming that the vorticity damping rate is small, the same amount of energy should be supplied to generate the compensating vorticity as for the formation of the main vorticity, but, since the energy is supplied via the work of the wall moving with a constant velocity C, the friction force on the wall should double.

In this case the liquid velocity at the free surface of the layer should closely coincide with the wall velocity. The same is true for the bubble. Therefore, the difference between the liquid and gas velocities at the free surface should be close to zero without friction, and the friction on the free surface can be neglected, i.e., it can be assumed that $\Delta p_2 = 0$ in Eq. (16) and that $K_g - K_f\theta = 0$ in Eq. (27).

To calculate the layer from Eq. (24), it is necessary to specify the initial condition (the fraction of the layer area a or a corresponding central angle α, see Fig. 1). This condition can be found by calculating the trailing front from the momentum and mass conservation equations. In the gravitational regime one may assume that a = 0.54 [11]. In the kinematic regime, the momenta equation is solved for the test liquid volume between sections 2 and 0 (Fig. 1) and has the form of Eq. (2) where $F_{fb} = F_{fc} = 0$, whereas the momentum flux is

$$F_{fd} = \rho_f V S (V_2 - \varkappa V), \tag{31}$$

where $\kappa = 1.36$ is the coefficient of momentum in section 0 passing through the plug in the case of turbulent flow.

The pressure drop across the plug cell will be obtained by summing Eqs. (15) and (16):

$$\Delta p_u = \lambda \frac{L_f}{D} \frac{\rho_f W^2}{2} + \rho_f W^2 \left(\frac{1}{\chi} - 1\right)^2 \left(\frac{1}{a_1} - \frac{1}{a_2}\right) + \tag{32}$$

$$+ (\rho_f - \rho_g) gD \cos\gamma (\Phi_1 - \Phi_2) + \Delta p_1 + \Delta p_2 + g \sin\gamma (\rho_f L_f + \rho_g L_g).$$

The first task of the present work was to find a convenient expression for the dimensionless pressure drop per unit tube length, i.e., to find a coefficient that differs from unity as little as possible and that admits a simple conversion into a dimensional pressure drop. Computational analysis has shown that the second and third terms on the right side of Eq. (32) amount to only 0.1-0.2 of the first term, whereas the fourth and the fifth terms constitute hundredths and thousandths of it. The sixth term disappears for horizontal tubes, while for small inclinations it is also very small in comparison with the first term. Therefore, Eq. (32) will be presented in the form

$$\Delta p_u = \lambda \frac{L_f}{D} \frac{\rho_f W^2}{2} (1 + \delta), \tag{33}$$

where $\delta << 1$.

A simple dimensionless expression is obtained by relating the pressure drop Δp_u to friction for a plug occupying the entire length of the cell L_u:

$$\Delta p_u \Big/ \left(\lambda \frac{L_u}{D} \frac{\rho_f W^2}{2}\right) = \frac{L_f}{L_u} (1 + \delta). \tag{34}$$

We express the ratio of the plug (L_f) to cell ($L_u = L_f + L_g$) lengths in terms of gas content. By definition, the true volumetric gas content is the ratio of the gas volume $(1 - \bar{a})SL_g$ in the cell to the volume $S(L_g + L_f)$ of the cell itself

$$\varphi = \frac{(1 - \bar{a}) L_g}{L_g + L_f}. \tag{35}$$

Hence,

$$\frac{L_f}{L_u} = 1 - \frac{\varphi}{1 - \bar{a}}. \tag{36}$$

Now, let us convert from the true volumetric to the flow-rate gas content. By neglecting the content of gas bubbles in the liquid, we obtain [10]

$$\beta = \varphi/\chi. \tag{37}$$

In order to convert from the length-mean cross-sectional area of the layer $\bar{a}$ to its length-mean velocity $\bar{\theta}$, use will be also made of Eq. (32) for the mass conservation law. Then Eqs. (36), (37), and (22) yield

$$\frac{L_f}{L_u} = 1 - \frac{1-\bar{\theta}}{1-\bar{\theta}/\chi}\beta = (1-\beta) - \bar{\theta}\beta\frac{1-\chi}{\chi-\bar{\theta}}. \tag{38}$$

In the limiting case of long layers and small gas densities, $\bar{\theta} \to 0$ and Eq. (38) gives

$$L_f/L_u = 1 - \beta. \tag{39}$$

Thus, dividing Eq. (34) by $(1 - \beta)$, one obtains the unknown dimensionless parameter which is close to unity for all the values of β and which admits a simple calculation of pressure drop Δp. Designating it by ψ, we have

$$\psi \equiv \Delta p \Big/ \left(\lambda \frac{L}{D}\frac{\rho_f W^2}{2}(1-\beta)\right). \tag{40}$$

The computational relation for the coefficient ψ follows from Eqs. (34), (39), and (40):

$$\psi = \left(1 - \bar{\theta}\frac{\beta}{1-\beta}\frac{1-\chi}{\chi-\bar{\theta}}\right)(1+\delta), \tag{41}$$

where

$$\delta = \frac{2}{\lambda(L_f/D)}\left(\left(\frac{1}{\chi}-1\right)^2\left(\frac{1}{a_1}-\frac{1}{a_2}\right) + \frac{(1-\rho)\cos\gamma}{\mathrm{Fr}}(\Phi_1 - \Phi_2) + \right. \tag{42}$$

$$\left. + \frac{\Delta p_1 + \Delta p_2}{\rho_f W^2} + \frac{\sin\gamma}{\mathrm{Fr}}\left(\frac{L_f}{D} + \rho\frac{L_g}{D}\right)\right).$$

The coefficient ψ in Eq. (41) is of the order of unity. The conversion to Δp from Eq. (40) is simple, since in addition to the quantities usually employed in hydraulic calculations of a single-phase fluid it requires only the assignment of the gas content β.

Figure 3 demonstrates the dependence of the coefficient ψ on β following [1, 4, 5, 6, 7, 8] and the lines of mean values. In [2, 3] the range of gas contents was narrow and, therefore, only the mean value of ψ was calculated. The parameters of the experiments are given in Table 1. The list of the mean experimental values of ψ for different values of β is given in Fig. 4. It is clear from this figure that, despite a wide range of Reynolds and Froude numbers, gas and liquid densities, tube diameters, media investigated, and experimental techniques, all the results virtually fall on one curve $\psi = \psi(\beta)$. The empirical formula for this curve has the form

$$\psi = 1 - 0.056\beta + 1.30\beta^2 - 1.44\beta^3 \tag{43}$$

is and the standard deviation of the data from the curve is 0.06. Such a close convergence of the results shows, first, that the data used are reliable and, second, that the total effect of all the factors on the coefficient ψ turns out to be weak.

Now, we compare experimental data with the calculation from Eqs. (41) and (42). The results of comparison are given in Fig. 5. Figure 5a shows the functions $\psi = \psi(\beta)$ calculated for the mean (from Table 1) parameters for four combinations of assumptions: 1) the friction of the layer against the wall is doubled, and there is no friction on the phase interface surface; 2) the friction of the layer against the wall is doubled, and the friction on the phase interface surface is determined from hydraulic relations; 3) the friction on the layer against the wall is not doubled, and there is no friction on the phase interface surface; 4) the friction of the layer against the wall and the friction on the phase interface surface are found from hydraulic relations. Curve 5 was plotted from Eq. (43) and depicts the experimental data. It is seen that the best fit with the experimental data is given by curve 1. The reasons for this were explained above. From Fig. 5a it is seen that the character of the assumptions about the friction on the phase interface surface has a weak effect on the function $\psi = \psi(\beta)$, whereas the assumptions about the layer friction against the wall have a rather strong effect (the discrepancies reach 30%).

The effect of the gas density (1, $\rho = 10^{-3}$; 2, $\rho = 10^{2}$; 3, $\rho = 3 \cdot 10^{-2}$; 4, $\rho = 10^{-1}$) on $\psi = \psi(\beta)$ is shown in Fig. 5b. The effect of the plug length (1, $L_f/D = 25$; 2, $L_f/D = 50$) is demonstrated in Fig. 5c, whereas Fig. 5d shows the effect of the Froude number (1, Fr = 1000; 2, Fr = 2). It is seen that the influence of all these factors (and also of the Reynolds number and roughness) is weak. This, probably, explains the fact that, despite a very wide range of experimental conditions (see Table 1), the data of all the authors closely coincide with one another (see Fig. 4).

From the computational analysis it is clear that the pressure drop coefficient is most sensitive to the relationship between the lengths of the gas bubble and of the liquid plug, which in the calculations depends on the character of the assumptions about the liquid layer (see Fig. 5a). The greater the friction of the layer against the wall, the faster (in moving coordinates) the acceleration of the layer and the smaller the fraction of the cross-sectional area of the tube it occupies. Then, the gas bubble occupies a large area and becomes shorter at the same gas content. The fraction of the bubble length in the plug cell falls and the fraction of the liquid plug grows. Since the pressure drop is determined in the main by the friction of the plug against the tube walls, the pressure drop per unit tube length also increases.

For plug flow in a tube with small inclinations and gradients (on the order of 0.03 and less) there is virtually no data on pressure drop (see, for example, reviews in [9, 18]). Recommendations for the calculation of pressure drop in inclined tubes reduce to the following: the friction force calculated for a horizontal tube should be supplemented by a longitudinal gravity component calculated from the density of the gas-liquid medium averaged by some means or other. However, this is not sufficient.

The change in the inclination alters not only the longitudinal component of gravity acting on a plug, which enters directly into the calculated pressure drop [see the last term in Eq. (42)], but also the gravity acting on the liquid layer. This changes the ratio of the bubble and plug lengths and, thus, affects the pressure drop per unit tube length (see Eq. (34)).

Figure 6a shows an example of the dependence of ψ on β calculated from the equations of the present paper for Fr = 10, $\gamma = +0.01$ (curve 1) and $\gamma = -0.01$ (curve 5). Curve 3 is plotted for $\gamma = 0$. Curves 2 and 4 depict the values of ψ which would have been obtained if from the value of ψ for $\gamma = \pm 0.01$ the quantity $\Delta\psi_f$ which is attributable to the gravity acting only on the plug was subtracted. It is seen that there is still a substantial difference in $\Delta\psi_g$ between curves 2 and 4 and the zero inclination curve 3. The difference is due to the action of gravity on the layer. The ratio $\delta\psi = \Delta\psi_g/\Delta\psi_f$ is given in Fig. 6b. It is seen to be comparable with unity.

The calculations have shown that at small angles γ of tube axis deviation from the horizontal, the quantity $\delta\psi$ is independent of γ, whereas the quantity $\Delta\psi = \psi - \psi(\gamma = 0)$ is proportional to sin γ. This means, in particular, that if the tube is slightly corrugated, then in calculations of hydraulic resistance for plug flow the corrugation can be neglected, since the slopes and gradients compensate one another.

LITERATURE CITED

1. A. A. Armand, Izv. VTI, No. 1, 16-23 (1946).
2. O. Baker, Oil Gas J., **53**, No. 12, 185-195 (1954).
3. P. B. Baksendell, in: Proceedings of the 4th Int. Oil Congress, Moscow (1956), pp. 332-339.
4. R. G. Reid et al., AIChE J., **3**, No. 3, 321-324 (1957).
5. V. E. Mukhin, Neftepromysl. Delo, No. 8, 30-33 (1975).
6. G. G. Kornilov, P. I. Chelpanov, and B. Ya. Zaretskii, Neftepromysl. Delo, No. 1, 21-24 (1976).

7. G. É.Odishariya, V. A. Mamaev, O. V. Klapchuk, and Yu. A. Tolasov, Two-Phase Transport of Oil and Gas [in Russian], Moscow (1977).
8. D. Ferre, Rev. Inst. Fr. Pet., **34**, No. 1, 113-142 (1979).
9. A. I. Guzhov, Simultaneous Extraction and Transport of Oil and Gas [in Russian], Moscow (1973).
10. G. Wallis, One-Dimensional Two-Phase Flows, McGraw-Hill, New York (1969).
11. É. É. Markovich, Inzh.-Fiz. Zh., **51**, No. 4, 680-685 (1986).
12. T. B. Benjamin, J. of Fluid Mech., **31**, pt. 2, 209-248 (1968).
13. V. A. Mamaev, G. É. Odishariya, N. N. Semenov, and A. A. Tochigin, Hydrodynamics of Gas-Liquid Mixtures in Tubes [in Russian], Moscow (1969).
14. A. K. Kazemipour and G. J. Apelt, J. Hydraul. Res., **20**, No. 3, 225-233 (1982).
15. J. Nikuradze, VDI-Forschungshelt, Göttingen (1926), p. 281.
16. H. Schlichting, Boundary-Layer Theory, McGraw-Hill, New York (1969).
17. O. N. Kashinskii and P. M. Krokovnyi, Prikl. Met. Tekh. Fiz., No. 4 (116), 74-78 (1979).
18. P. L. Spedding, J. J. Chen, and V. T. Nguen, Int. J. Multiphase Flow, **8**, No. 4, 407-431 (1982).

HYDRAULIC RESISTANCE AND HEAT TRANSFER IN LONGITUDINAL FLOW PAST STAGGERED TUBE BUNDLES WITH WALLS OF DIVERGENT-CONVERGENT PROFILE

F. V. Vasil'ev and V. T. Buglaev

UDC 536.242

The results of an experimental investigation into the effect of the characteristic dimensions of staggered convergent-divergent tube bundles on hydraulic resistance and heat transfer in a longitudinal flow are presented.

As before, the enhancement of heat transfer in different-purpose tubular heat exchangers remains an urgent applied problem in the theory of heat and mass transfer [1-5].

In the case of the single-phase heat carrier transverse flow past tube bundles, the problem of heat transfer enhancement is usually unambiguously solved by applying finned tubes, because the use of different types of turbulizers, just as the change in the shape of the walls, does not give desirable positive results as compared with smooth-wall tube bundles [3-5].

By the present time, the most developed and verified method for the enhancement of heat transfers is during the turbulent flow of various heat carriers in tubes with different types of turbulizers or with the shape and geometric dimensions of the cross section varying along the flow path. The relevant literature contains voluminous information relating to the thermo-hydraulic characteristics of heat-exchanging tubes with annular knurling [1], helical tubes [2, 6], tubes with a divergent-convergent profile [7-10], etc. This has made it possible to start a wide practical incorporation of tubes with heat transfer amplifiers into real heat exchangers with a substantial improvement in their characteristics.

As a rule, the application of turbulization mechanisms to the internal walls of tubes leads inevitably to the deformation of the outer walls. The question then naturally arises as to the estimation of the extent of heat transfer intensification on these walls in the case of longitudinal flow past tube bundles. This attempt was made in a comprehensive study [2] where the characteristics of the ovally-coiled tubes that ensured heat transfer enhancement both in tube and intertube space were investigated. However, the gain in energy with the use of ovally-coiled tubes is relatively small, while they are very difficult to manufacture and have insufficiently reliable strength characteristics.

Bryansk Institute of of Transport Machine Building. Translated from Inzhenerno-Fizicheskii Zhurnal, Vol. 62, No. 6, pp. 803-807, June, 1992. Original paper submitted May 27, 1991.

1062-0125/92/6206-0578$12.50 ©1992 Plenum Publishing Corporation